Indian Journal of Chemical Technology
Vol. 29, November 2022, pp. 697-705
DOI: 10.56042/ijct.v29i6.67350

Development of silver nanoparticle stabilized poly (aniline -co- pyrrole) for electrochemical application

E Murugan*, F Lyric, K Janakiraman, S Saranya & M Kaviya Sri
Department of Physical Chemistry, School of Chemical Sciences, University of Madras, Guindy Campus, Chennai 600 025, Tamil Nadu, India.
E-mail: dr.e.murugan@gmail.com

Received: *19 August 2022; accepted*: *21 October 2022*

Silver nanoparticles (Ag-Nps) decorated conducting copolymers of aniline and pyrrole monomers [poly (aniline -co-pyrrole)] have been synthesized through a simple *in-situ* chemical oxidative co-polymerization. The formation and characteristics of poly (aniline -co- pyrrole)-Ag have been confirmed using microscopic and spectroscopic techniques. The synthesized nanocomposite has been characterized using scanning electron microscopy, fourier transform infra-red spectroscopy, RAMAN spectroscopy, X-ray diffraction, thermogravimetric analysis and UV-Visible spectroscopy have been used to identify the phase, morphology and thermal stability. The composite has been used to modify the glassy carbon electrode to obtain poly (aniline -co- pyrrole)-Ag/ GCE. Cyclic voltammetry and square wave voltammetry have been used for the electrochemical sensing of uric acid. The modified GC electrode has shown an excellent electrocatalytic oxidation of uric acid to allantoin at neutral pH of phosphate buffer solution. The proposed sensor thus involves simple fabrication with high accuracy and sensitivity.

Keywords: Ag-Nps, Poly (aniline -co-pyrrole), Sensors, Uric acid

2,4,6 – Trihydroxy purine (uric acid), an end product of the purine metabolism, is present in biological fluids in the form of urine and serum at a range of 200–450 μM[1]. The elevated level of uric acid is indicated by diseases such as arthritis, gout, metabolic syndrome, hypertension and cardiovascular disorder whereas, hypouricemia (*i.e*)., low level of uric acid in the human body, may direct to Parkinson's disease. Hence, balance of uric acid in biological matrices is an important sign in human physiological processes[2]. Consequently, precise estimation of urate level is significant in the early stage of diagnosis and therapy. Accordingly for fast response, simple method and accurate assessment, the electrochemical approach has been preferred among various analytical techniques[3]. However, due to the overlapping of the oxidation potential of uric acid to that of the bare electrode, the explicit determination of uric acid is vital. Therefore, it is essential to fabricate electrodes that are more sensitive towards uric acid analyte than the glassy carbon electrode[4].

Subsequently, to pick a foremost electrocatalyst with great influence in view of its stability, charge transfer and reproducibility is formidable[5-10].UA sensors have been designed by modifying the electrode surface through polymer-based materials, binary or ternary nanocomposites, biological molecules etc[11]. Recently, polyaniline/ironoxide-tin oxide/reduced graphene oxide, 2D-titanium carbide (MXene), silver doped iron oxide nanocomposite coupled with polyaniline, Ag-doped PANI nanocomposites, gold nanoparticles on polyaniline, $CuBi_2O_4$ films, Co_3O_4-ERGO nanocomposite, metal-organic frameworks have got fascinating recognition among researchers in electrochemical studies[12-18]. Amidst these materials, conducting polymers have come to light in the sensing platform to meet the high demands for electrochemical detection[19-24].

The preamble of conducting polymers has been due to the intense physical and electroconductive property that can essentially transfer electric charge produced during a biochemical reaction[25]. Generally, conducting polymers such as PANI, polypyrrole (Ppy), and poly(3,4-ethylenedioxythiophene) (PEDOT) are widely accepted for electrochemical applications on account of their distinct properties[26]. Among which, PANI and Ppy have supercilious consideration due to their π conjugated electron systems, that promote molecule immobilization owing to the groups that are present in the polymer structure that are oppositely charged to those that are present in the detected analyte[27]. Polyaniline is well known for its non-toxicity, low cost, highly conductive, corrosion resistant as well as pronounced shelf life of the electrodes with intense redox properties[28]. Similarly,

Ppycontributes speed, accuracy especially to anionic species like urate and ascorbate because of its sensitivity against the interferents present in the medium[29]. Moreover, conducting polymers are very promising materials for bioanalytical application (designing a biosensor, for rechargeable batteries, corrosion prevention, fuel cell, supercapacitors, microwave absorption[30-35] etc.)

Co-polymerization is known to be an easy and powerful method for obtaining polymer with desired properties, and are thus widely used in the production of commercial polymers including fundamental investigation of structural-property relationships[36]. Eventually, to enhance the stability of the copolymer, it is often functionalized or incorporated with nanoparticles. In this study, silver nanoparticles were doped on to poly(aniline-copyrrole). It has excellent electrical conductivity that paves way for efficient electron transfer with good surface area[37]. So, silver nanoparticles based electrochemical sensors are suggested for the detection of uric acid. Though there were many reports for electrochmeical sensing of uric acid using polyaniline, polypyrrole and silver decorated polyaniline and polypyrrole separately, the composite derived using poly(aniline-co-pyrrole) and silver nanoparticle has not been attempted so far. The copolymer is also conducting well and hence it can very well capture electrons from the analyte and transfer the same to the electrode. Thus, in this present work aniline and pyrrole were copolymerized by oxidative chemical copolymerization for the immobilization of silver nanoparticles. Then poly(aniline-co-pyrrole)/AgNps were characterized using Fourier transform infrared spectroscopy (FTIR), scanning electron microscopy (SEM), RAMAN, UV–Visible spectroscopy and XRD, and the as-synthesized nanocomposites were pasted on GCE to obtain the Poly(Aniline-co-pyrrole)/AgNps/GCE. The efficiency of the modified GCE was tested for the electrocatalytic oxidation of Uric acid through cyclic voltammetry (CV) and square wave voltammetry (SWV). The fabricated sensor showed low limit of detection (LOD) equal to 0.953 μM. The results showed high Electrocatalytic behaviour for poly(aniline-co-pyrrole)/AgNps/GCE under experimental conditions.

Experimental Section

Materials

Silver nitrate ($AgNO_3$), Sodium carbonate (Na_2CO_3), aniline ($C_6H_5NH_2$), pyrrole (C_4H_5N), ammonium per sulphate ($(NH_4)_2S_2O_8$), sodium borohydride ($NaBH_4$), hydrochloric acid, uric acid was purchased from Sigma-Aldrich and used as received. A phosphate buffer solution (PBS) of different pH was prepared with appropriate amounts of sodium phosphate monobasic dihydrate ($NaH_2PO_4.2H_2O$), sodium phosphate dibasic dihydrate ($Na_2HPO_4.2H_2O$), and adjusted with 0.1 M (phosphoric acid) H_3PO_4 or sodium hydroxide (NaOH). All other chemicals used were of analytical grade.

Preparation of poly(Aniline-co-Pyrrole)/AgNps

The poly(aniline-co-pyrrole)/AgNps were prepared through an *in situ* chemical oxidative polymerization of aniline and pyrrole monomers at 1:1 molar ratio. Initially, 0.01M of the monomers were dispersed in 0.1M HCl at 0-5°C under vigorous stirring for 1 h to obtain a uniform mixture. To the above mixture 25 mL of aqueous ammonium persulphate was added dropwise to initiate polymerization. The reaction was maintained at 0°C for 12h. The powdered precipitate was filtered and washed several times with distilled water until a neutral pH was reached for the filtrate. The moist precipitate on drying yielded the poly(aniline-co-pyrrole). The synthesis of the conducting copolymer is shown in Fig. 1. However, for the preparation of poly(aniline-co-pyrrole)/AgNps, the moist precipitate was dispersed in 100 mL of distilled water to which 0.01 M of $AgNO_3$ was added dropwise. It was stirred for 1 h and the solution is labelled A. Then, 0.01 M $NaBH_4$ was labelled solution B, was added in drops to solution A and the stirring continued for 3h. Ultimately the prepared composite was centrifuged, washed with distilled water and ethanol followed by drying at 60°C overnight.

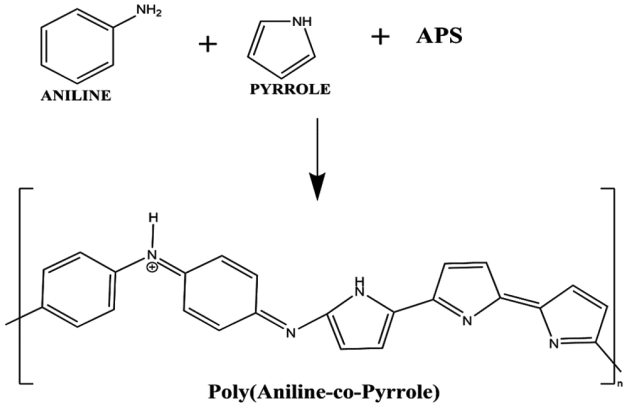

Fig. 1—Synthesis of the conducting copolymer [poly(aniline-co-pyrrole).

Fabrication of Poly(aniline-co-pyrrole)/Ag on to GC electrode

Preceding to the modification of the glassy carbon electrode, the nanocomposite was initially dispersed in ethanol and ultrasonicated. After dispersion, about 5 µL of the composite was drop casted on to the GC electrode. Thus, the acquired modified GCE was dried at room temperature. Eventually, the modified GCE was used for electrochemical determination of uric acid. Figure 2 exhibits the schematic representation for the synthesis and fabrication of Poly(aniline-co-pyrrole)/Ag nanocomposite on glassy carbon electrode.

Results and Discussion

Characteristics of morphology

Figures 3(a) and 3(b) display the morphology of poly(aniline-co-pyrrole). The average particle size

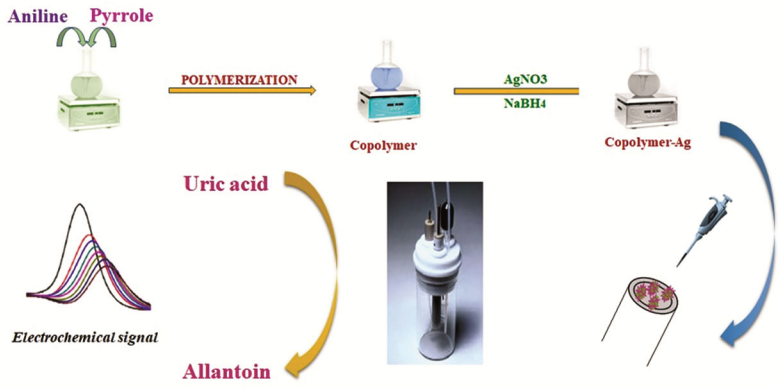

Fig. 2—Schematic representation for the synthesis of poly(aniline-co-pyrrole)/Ag/GCE.

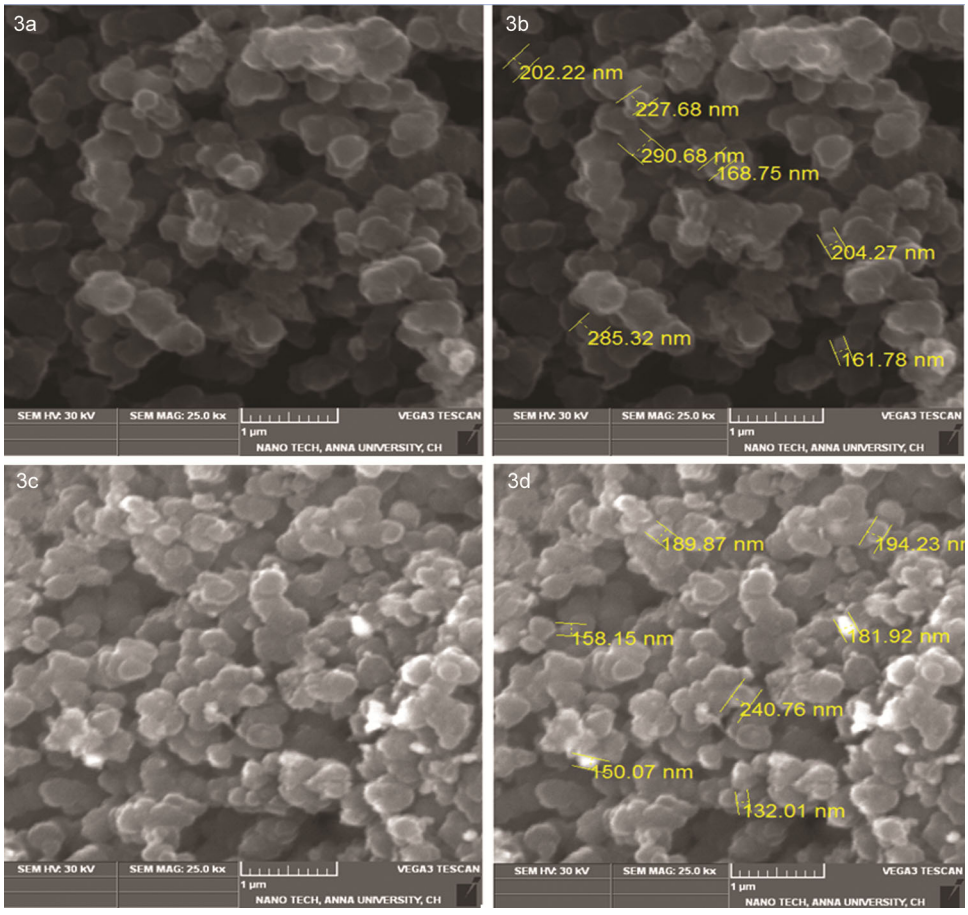

Fig. 3—SEM image of (a & b) poly(aniline-co-pyrrole) and(c & d) poly(aniline-co-pyrrole)/Ag.

varied from 200-225 nm. The SEM images of poly-(aniline-co-pyrrole)/AgNps are shown in Figs 3(c) and 3(d), the light spots correspond to the silver nanopartcle while the dark ones are the copolymer matrix. This confirms the fabrication of silver nanoparticles on to the copolymer units.

FT-IR Spectroscopy

The FT-IR spectra of poly(aniline-co-pyrrole) and Poly(aniline-co-pyrrole)/AgNps are shown in Fig. 4. The peaks at 3734 and 3427 cm^{-1} are due to N-H stretching vibrations. The C=N yielded a sharp intense peak at 1573 cm^{-1}. The C-N vibration occurred at 1384 cm^{-1}. The group of peaks between 1000 and 1300 cm^{-1} are due to N-H bending and pyrrole ring vibrations. The peaks below 1000 cm^{-1} are due to aromatic -CH bending vibrations. The FT-IR spectrum of poly(aniline-co-pyrrole)/AgNps showed more intense peaks, particularly C=N and N-H stretching vibrations, than the poly(aniline-co-pyrrole). The incorporation of Ag nanoparticle facilitates extension of quinonoid chains and so the intensity of the peak at 1579 cm^{-1} increased. But the peak is shifted towards higher energy than that of poly(aniline-co-pyrrole). It indicates bonding of pyrrole nitrogen lone pair with silver nanoparticles. Such bonding decreases nitrogen lone pair delocalization and strengthening the bond of quinonoid rings.

X-ray diffraction (XRD) analysis

The X-ray diffraction pattern of poly(aniline-co-pyrrole)/Ag is shown in Fig. 5. The peaks at 2θ=37.0°, 43.1°, 62.8° and 74.9°are due to silver nanoparticles, and they are indexed to (111), (200), (220) and (311). The peak at 29.3°2θ is due to the polymer.

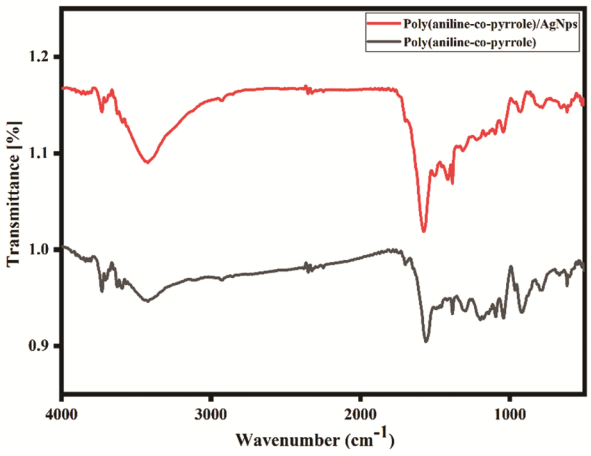

Fig. 4—FT-IR spectrum of poly(aniline-co-pyrrole) and poly(aniline-co-pyrrole)/Ag.

Raman spectral studies

The raman spectra of poly(aniline-co-pyrrole) and poly(aniline-co-pyrrole)/Ag are shown in Fig. 6. The peaks at 1364 and 1556 cm^{-1} are due to C-N and C=N vibrations of the polymer chain. A peak around 600 cm^{-1} appeared in the composite but not in the copolymer, it is due to the activation of C-H bending vibration by silver nanoparticles. The increase in the

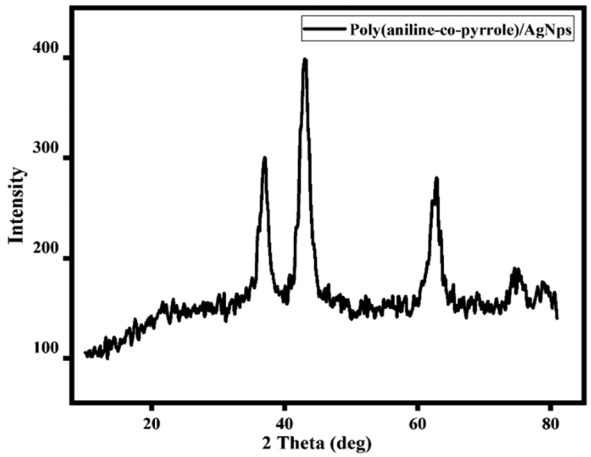

Fig. 5—X-ray diffraction pattern of Poly(aniline-co-pyrrole)/Ag.

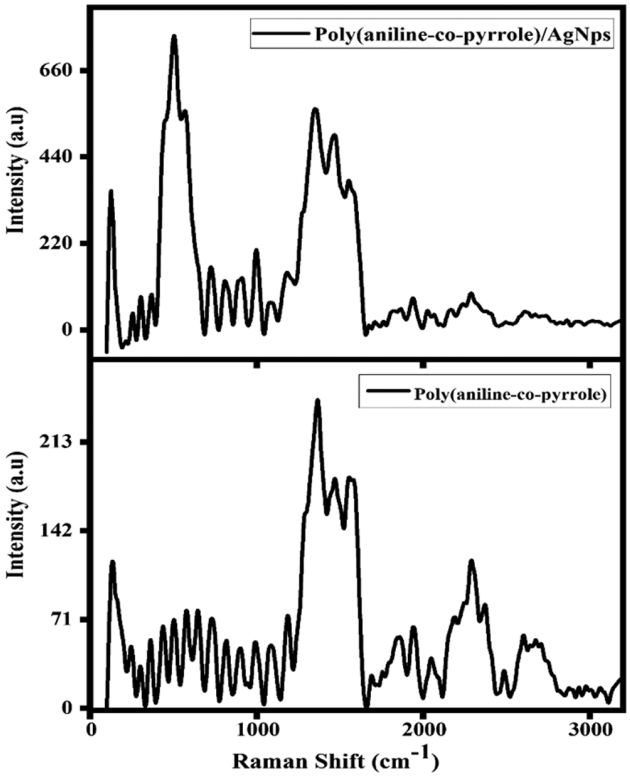

Fig. 6—Raman Spectra of Poly(aniline-co-pyrrole) and Poly(aniline-co-pyrrole)/Ag.

intensity of the peaks between 1100 – 1800 cm^{-1} of the composite illustrates extensive delocalization of the π electronic cloud due to the addition of silver nanoparticles, as discussed in the FT-IR analysis.

UV-Visible spectra

The UV – Visible spectra of Poly(aniline-co-pyrrole)/Ag is shown in Fig. 7. The absorbance extends from near infrared to the end of visible region. It is due to π-π* transition in the composite. It confirms conjugation of the quinonoid rings.

TGA studies

The results of the thermogravimetric analysis of the composite are shown in Fig. 8. The analysis was carried out between 25 and 500°C in nitrogen at a heating rate of 1°C/min. The initial weight loss below 100°C is due to the desorption of water. The subsequent weight loss which started around 150°C is due to the degradation and desorption of the polymer. The degradation occurred from 150 – 500°C.

Electrocatalytic activity of poly(aniline-co-pyrrole)/Ag for the detection of uric acid

The square wave voltammetry and cyclic voltammetry were applied for the electrochemical detection of UA using the composite modified GC electrode and the corresponding electron transfer mechanism for the oxidation of uric acid is represented in Fig. 9. The analysis was carried out at *p*H 5.8-8.5 in a phosphate buffer medium. On comparing the voltammograms for with and without the analyte it was observed that modified Poly(aniline-co-pyrrole)/Ag/GCE, with and without uric acid at *p*H 7, the oxidation current of poly(aniline-co-pyrrole)/Ag/GCE with uric acid was higher than that of the modified electrode without uric acid. The corresponding cyclic voltammo-grams are shown in Fig. 10. This confirms that Poly(aniline-co-pyrrole)/Ag/GCE as active towards the oxidation of uric acid.

Effect of *p*H

The effect of *p*H on the electrochemical behaviour of uric acid on poly(aniline-co-pyrrole)/Ag/GCE was

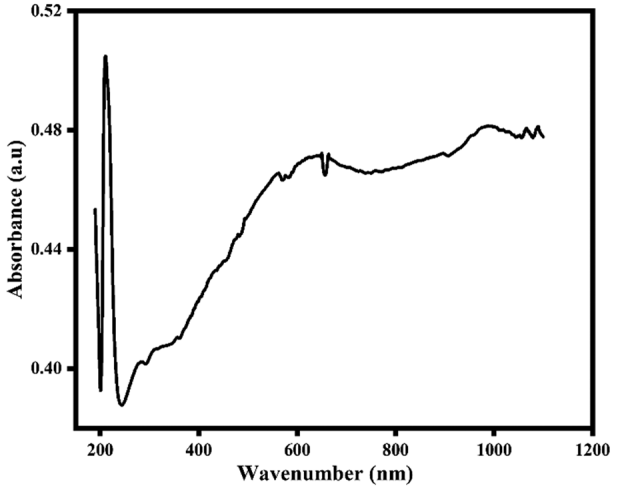

Fig. 7—UV-Visible spectrum of poly(aniline-co-pyrrole)/Ag.

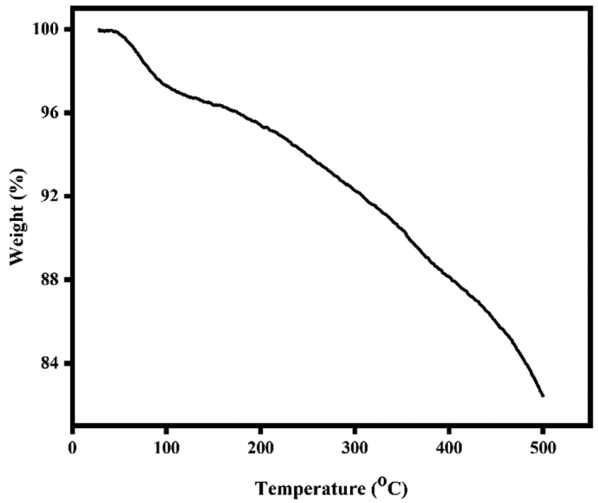

Fig. 8—GA plot of poly(aniline-co-pyrrole)/Ag.

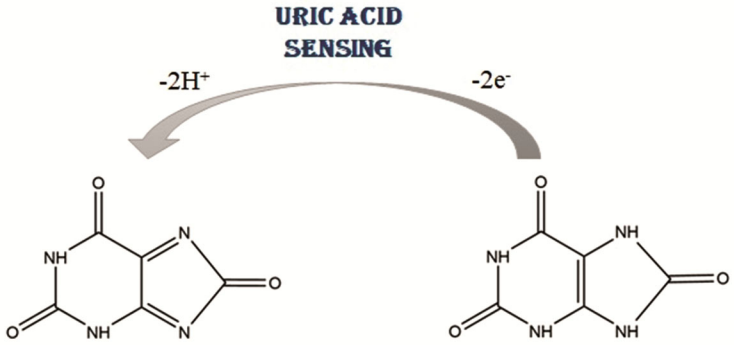

Fig. 9—Electrochemical oxidation of uric acid.

monitored from 5.8 – 8.5 and the results are shown in Fig. 11. An intense oxidation peak was observed at *p*H 7 at a lower potential of 0.6V. The oxidation of uric acid does not occur with equal number of proton and electron transfer at poly(aniline-co-pyrrole)/ Ag/GCE. It was confirmed by the Nernstian slope value at -14 mV. For the plot of pH versus Epa at 0.1M PBS, the linear regression equation is:

$E^{o}_{1/2}$ (mV) = -14 + 0.70908 (correlation coefficient γ = 0.9884) … (1)

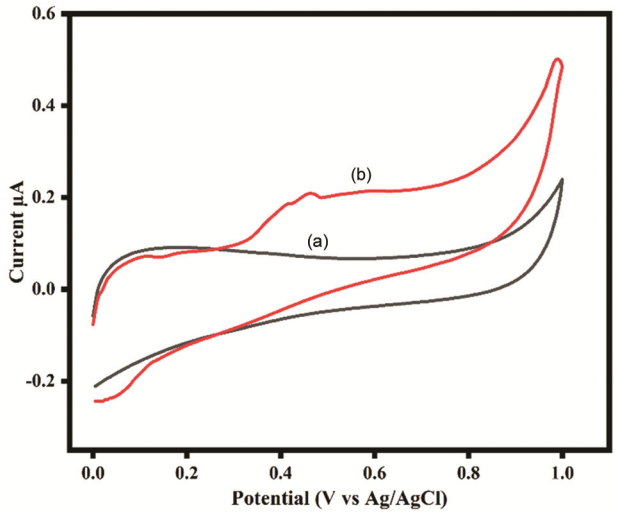

Fig. 10 — Cyclic voltagramms of (a) Poly(aniline-co-pyrrole)/Ag and (b)1 mM UA at poly(aniline-co-pyrrole)/Ag/GCE. Scan rate: 50 mV/s (PBS=0.1M, *p*H: 7).

Effect of scan rate

Scan rate for the electrochemical oxidation of uric acid on poly(aniline-co-pyrrole)/Ag/GCE was examined through CV and the cyclic voltammograms are shown in Fig. 12. The oxidaion current increases with increase in scan rate from 5–700 mV. The linear relationship for the double logrithimic plot between frequency and current at 0.1M PBS suggests that the reaction is adsorption controlled with slope vaule is 0.77574. It followed the following linear regression equation:

$Ip_a = 3.67387x10^{-7} (v^{1/2}) + 6.86627$ ($R^2 = 0.99465$) ... (2)

Effect of concentration

The electrochemical oxidation of uric acid was carried out for bare GCE as well as for poly(aniline-co-pyrrole)/Ag/GCE in 0.1M PBS at a scan rate of 50 mVs^{-1}. The corresponding cyclic voltammograms are shown in Fig. 13. No peak was observed for the bare

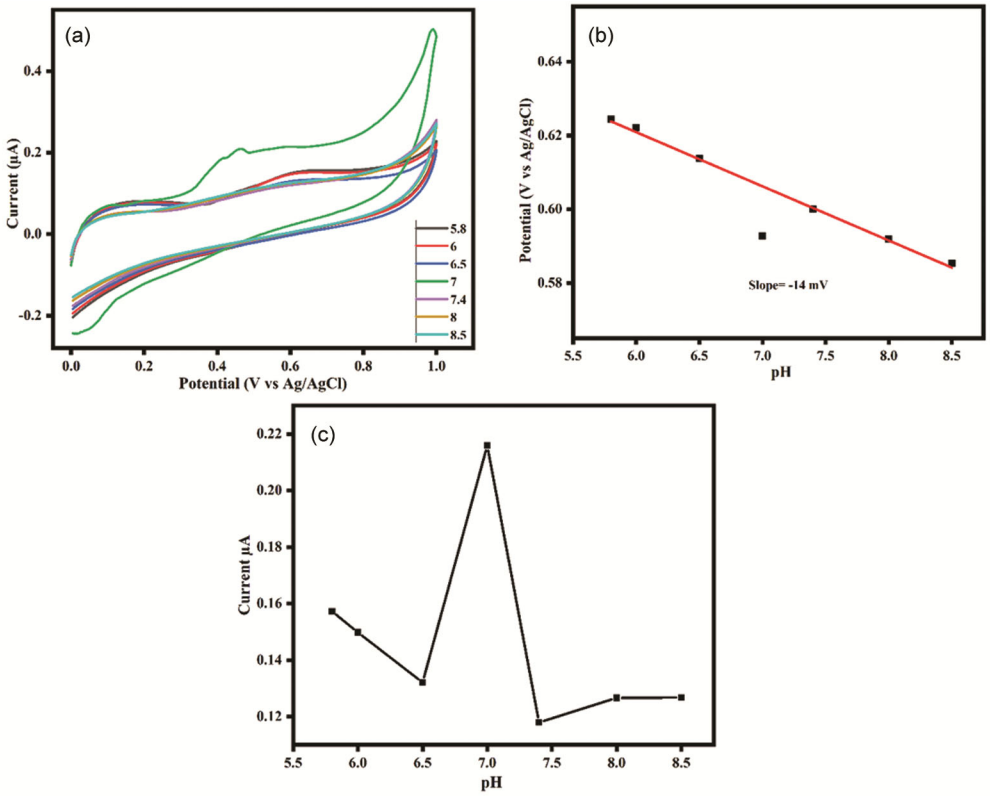

Fig. 11 — Cyclic voltammogram for the oxidation of uric acid with poly(aniline-co-pyrrole)/Ag in 0.1M PBS at different *p*H; (b) Plot of $E_{1/2}$ of Ep versus *p*H and (c) Plot of *p*H versus peak current.

GC electrode. Thus, to overcome this poor electrochemical activity, the modified GCE was used. At the anodic peak potential 0.6 V, the oxidation current increased with increase in the concentration of uric acid and the linear concentration range was found to be 0.6622–7.975 µM whose limit of detection (LOD) and limit of quantification (LOQ) was equal to 0.953 µM and 3.177 µM, respectively with a sensitivity 0.0873 µA/µM.

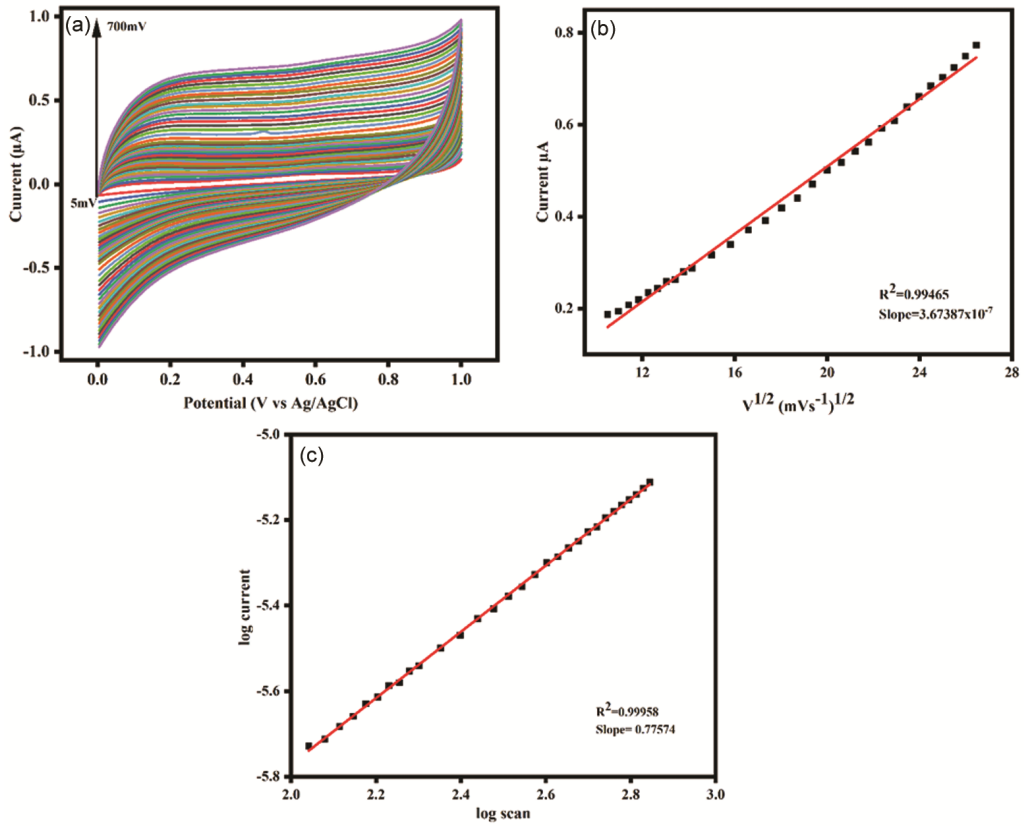

Fig.12 — Effect of scan rate for the oxidation of uric acid (PBS: 0.1M; *p*H: 7) with poly(aniline-co-pyrrole)/Ag; (b) Plot of oxidation peak current versus square root of scan rate and (c) Double logrithimic plot of logv versus log Ip.

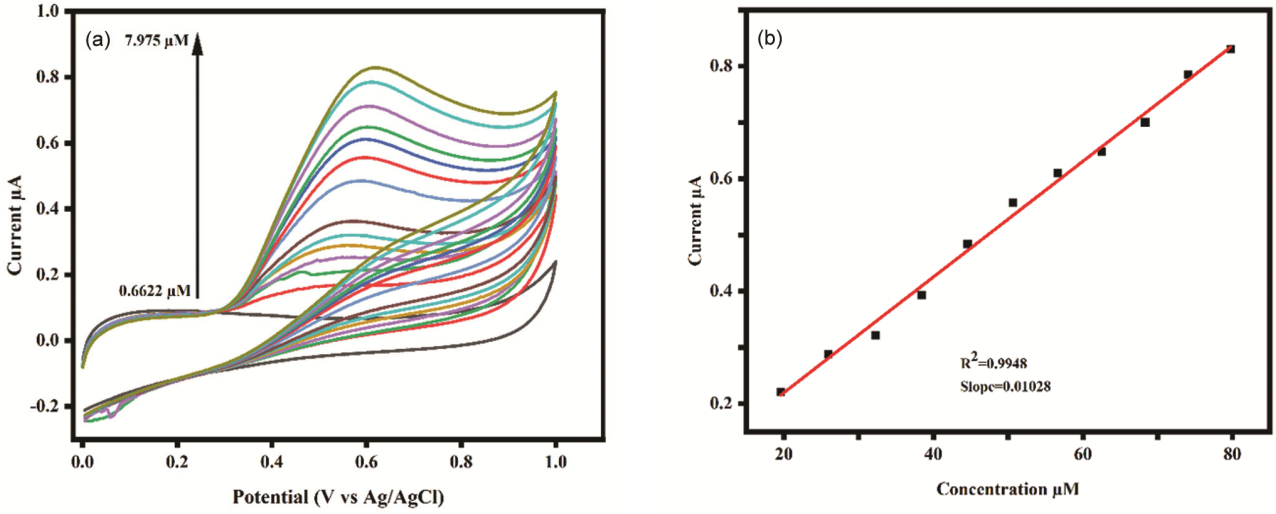

Fig. 13 — Cyclic voltagramms for the oxidation of uric acid with poly(aniline-co-pyrrole)/Ag at different concentrations PBS: 0.1M; Scan rate: 50 mVs^{-1} and (b) Calibration plot for concentration versus Current.

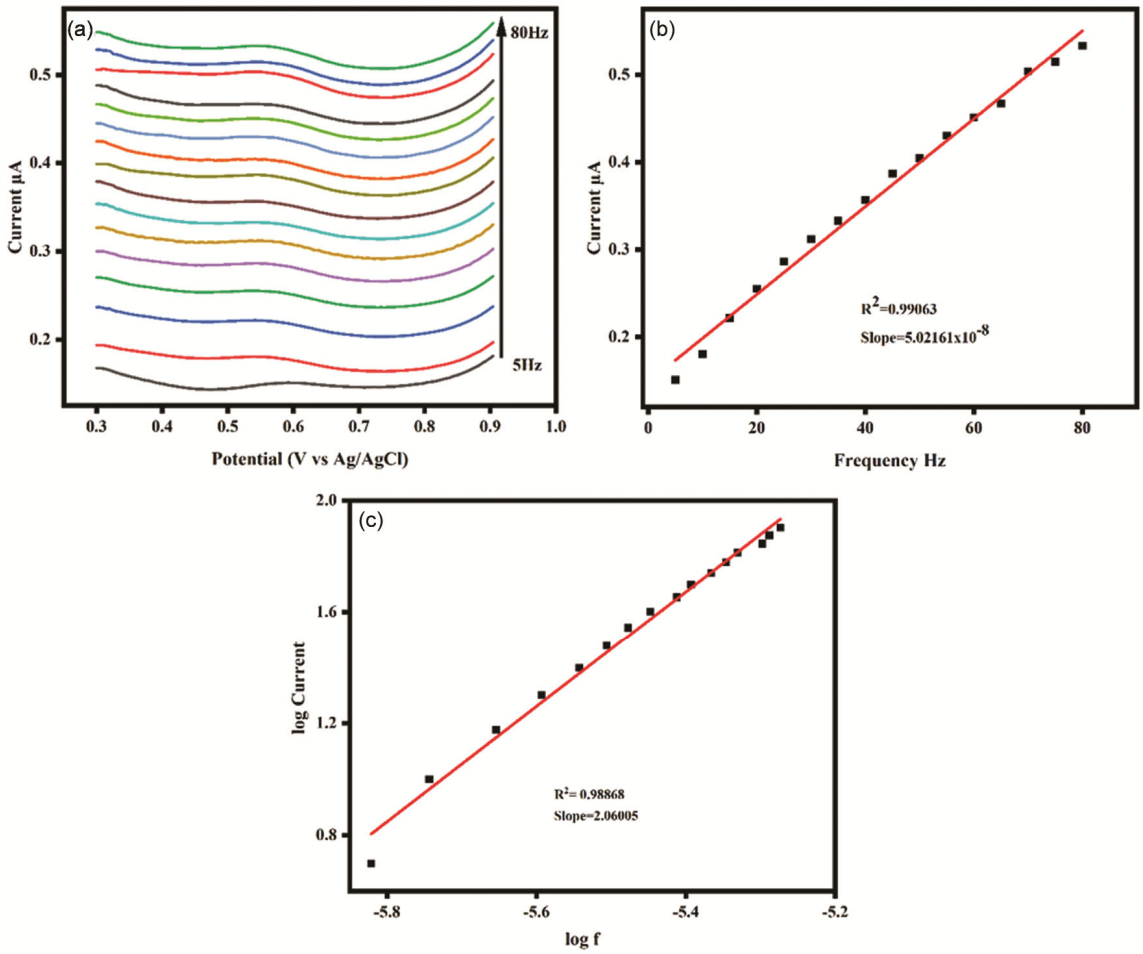

Fig. 14—(a) Effect of frequency for the oxidation of uric acid (PBS: 0.1M; pH: 7) with poly(aniline-co-pyrrole)/Ag; (b) Plot of oxidation peak current versus frequency and (c) Double logrithimic plot of logf versus. log Ip

Effect of frequency

The square wave voltammetric technique was utilized for evaluating the elctrochemical behaviour of uric acid on poly(aniline-co-pyrrole)/Ag/GCE. With increase in frequency from 5 – 80 Hz the resulting square wave voltagramms for the modified electrode are shown in Fig. 14. On increasing the frequency there is an increase in the anodic peak current. The linear relationship between log f and log current proves that the reaction is adsorption controlled with a slope 2.0600. The resulting linear regression equation is:

$$Ip_a = 5.02161x10^{-8}\, V^{1/2} + 1.4832x10^{-6}\ (R^2 = 0.99063) \ldots (3)$$

Conclusion

Silver nanoparticles decorated co-polymer has been synthesized through *in situ* chemical oxidation with aniline and pyrrole monomers. Time saving, simple pretreatment procedures have been used for the modification of GC electrode. It established accurate assesment with favourable electrocatalytic performance for the detection of uric acid. After arriving at the optimum condition, poly(aniline-co-pyrrole)/Ag/GCE provided a linear range of 0.6622–7.975 µM. From the linear regression equation, it is verified that the electrochemical determination of uric acid is adsorption controlled whose R^2 and slope values were 0.99958 and 0.77574, respectively. Thus, the modified electrode could be exploited for the elctrochemical sensing of other active components of biological fluids.

Acknowledgement

The authors are grateful for the financial support provided by University Research Fellowship (URF) and Rashtriya Uchchatar Shiksha Abhiyan (RUSA) 2.0 RI & QI.

References

1 Sathish Kumar Ponnaiah, Prakash Periakaruppan & Balakumar Vellaichamy, *J Phys Chem B*, (2018).

2 Tingfan Tang, Menglin Zhou, JiapeiLV, Hao Cheng, Huaisheng Wang, Danfeng Qin, Guangzhi Hu &Xiaoyan Liu, *Colloids Surf B: Biointerfaces*, 216 (2022) 112538.

3 Kai Ma, Luoxing Yang, Jun Liu & Jiyang Liu, *Nanomaterials*, 12 (2022) 1157.

4 Hemin Wang, Chunying Xu & Baiqing Yuan, *Int J Electrochem Sci*, 14 (2019) 8760.

5 Murugan E, Rani D P G & Yogaraj V, *Colloids Surf B: Biointerfaces*,114 (2014) 121.

6 Murugan E, Priya A R J, Raman K J, Kalpana K, Akshata C R, Kumar S S & Govindaraju S, *J Nanosci Nanotechnol*, 19 (2019) 7596.

7 Murugan E & Rangasamy R, *J Biomed Nanotechnol*, 7 (2011) 225.

8 Murugan E & Gopinath P, *J Mol CatalA Chem*, 294 (2008) 68.

9 Murugan E & Shanmugam P, *J Nanosci Nanotechnol*, 16 (2016) 426.

10 Murugan E, Akshata C R, Yogaraj V, Sudhandiran G & Babu D, *Ceram Int*, 48 (2022) 16000.

11 Paulraj P, Ahmad Umar K, Rajendran A, Manikandan R, Kumar E, Manikandan K, Pandian Mater H, Mahnashi Mabkhoot A, Alsaiari Ahmed A, Ibrahim Nikolaos Bouropoulos S & Baskoutas, *Electrochim Acta*, 363 (2020) 137158.

12 Daria Minta, Adam Moyseowicz, Stanisław Gryglewicz & Grazyna Gryglewicz, *Molecules*, 25 (2020) 5869.

13 Murugan N, Jerome R, Preethika M, Sundaramurthy Anandhakumar, Sundramoorthy Ashok K, *J Mater Sci Technol*, 72 (2021) 122.

14 Sathish Kumar Ponnaiah, Prakash Periakaruppan & Balakumar Vellaichamy, *J Phys Chem B*, 122(2018) 3037.

15 Mahalakshmi S & Sridevi V, *Electrocatalysis*, 12 (2021) 415.

16 Cheng-HsienWu, Emeline Onno & Chia-Yu Lin, *Electrochim Acta*, 229 (2017) 129.

17 GizemTurkkan, Salih Zeki Bas, KezibanAtacan & Mustafa Ozmen, *Anal Methods*, 14 (2022) 67.

18 Qodratollah Azizpour Moallem & Hadi Beitollahi, *Microchem J,* 177 (2022) 107261.

19 Siva A & Murugan E, *Synthesis*, 17 (2005) 2927.

20 Yogaraj V, Gowtham G, Akshata C R, Manikandan R, Murugan E & Arumugam M, *J Drug Deliv Sci Technol*, 58 (2020) 101785.

21 Murugan E, Nimita J, Ariraman M, Rajendran S, Kathirvel J, Akshata C R & Kumar K, *ACS Omega*, 3 (2018) 13685.

22 Murugan E & Shanmugam P, *Bull Mater Sci*, 38 (2015) 629.

23 Murugan E, Govindaraju S & Santhoshkumar S, *Electrochim Acta*, 392 (2021) 138973.

24 Murugan E, Rani D P G, Srinivasan K & Muthumary J, *Expert Opin Drug Deliv,*10 (2013) 1319.

25 Mishra Shreshtha S, Ghodki Nandita V, Chopra Swamini, Pande S A, Deshmukh Kavita A, Deshmukh Abhay D & Peshwe D R, *IJSRM*, 8 (2017).

26 Javad Hosseini, Ehsan Nazarzadeh Zare & Davood Ajloo, *J Mol Liq*, 296 (2019) 111789.

27 Xua P, Hana X J, Wanga C, Zhanga B & Wang H L, *Synth Met*, 159 (2009) 430.

28 YeetHoong Changa, Pei Meng Woia & Yatimah Alias, *Microchem J*, 148 (2019) 322.

29 Solanki Pratima R, Singh Suman, Prabhakar Nirmal, Pandey M K & Malhotra B D, *J Appl Polym Sci*, 105 (2007) 3211.

30 Chao Zhang, Saravanan Govindaraju, Krishnan Giribabu, Yun Suk Huh & Kyusik Yun, *Sens Actuators B Chem*, 252 (2017) 616.

31 Shilun Gao, Feiyuan Sun, Nian Liu, Huabin Yang & Peng-Fei Cao, *Mater Today*, 40(2020) 140.

32 YijieJin, Zhihao Chen, Wenzhong Yang, Xiaoshuang Yin, Yun Chen & Ying Liu, *J Taiwan Inst Chem Eng*, 117 (2020) 171.

33 Prasanta Pattanayak, Farhan Papiya, Vikash Kumar, Amandeep Singh & PatitPaban Kundu, *Mater Sci Eng*, 118 (2021) 111492.

34 Banglei Liang, Zongyi Qin, Tao Li, Zhenjun Dou, Fanxin Zeng, Yameng Cai, Meifang Zhu & Zhe Zhou, *Electrochim Acta*, 177 (2015) 335.

35 Yao-Feng Zhu, Li Zhang, Toshiaki Natsuki, Ya-Qin Fu & Qing-Qing Ni, *Synth Met,* 162 (2012) 337.

36 Bo Liu, Hongjuan Sun, Tongjiang Peng & Xin Zhi, *Diam Relat Mater*, 118 (2021) 108498.

37 Mota María L, Carrillo Amanda, Verdugo Ana J, Olivas Amelia, Guerrero Jorge M, De la Cruz Edna C & Ramírez Natalia Noriega, *Molecules*, 24 (2019) 1621.